MINISTERE DE L'ENSEIGNEMENT SUPERIEUR ET DE LA RECHERCHE SCIENTIFIQUE

Felix Houphouet-Boigny University

N°: 670

UNITE DE FORMATION ET DE RECHERCHE SCIENCES DES STRUCTURES DE LA MATIERE ET DE TECHNOLOGIE

RÉPUBLIQUE DE CÔTE D'IVOIRE

UNION - DISCIPLINE - TRAVAIL

Steel Institute of RWTH Aachen University

SPONSORED BY THE Federal Ministry of Education and Research

MASTER IN RENEWABLE ENERGY AND CLIMATE CHANGE

SPECIALITY: PRODUCTION AND TECHNOLOGY OF GREEN HYDROGEN

Topic:

EXPLORING HIGH-STRENGTH STEEL PERFORMANCE FOR SUSTAINABLE HYDROGEN ENERGY STORAGE AND TRANSPORT

Presented on the 29th September 2023 by

Abdallah KEZIRE

Jury:

Prof. KOUADIO Yves	**President**
Dr. TILLOUS Eric (MC)	**Examiner**
Dr. FASSINOU Wanignon Ferdinand (MC)	**Major Supervisor**
Prof. Dr.-Ing. Ulrich Krupp	**Co-Supervisor**

Academic year: 2022-2023

"To my beloved family,

This work stands as a testament to the unwavering support, love, and guidance you have bestowed upon me throughout my journey. Your sacrifices and encouragement have been the driving force behind my accomplishments. With profound gratitude, I dedicate this work to you, as a small token of my love and appreciation.

With all my love,
Abdallah KEZIRE"

FOREWORD AND ACKNOWLEDGMENTS

I would like to extend my heartfelt gratitude to the following individuals and institutions whose support and contributions have been instrumental in making my academic journey a success:

I am thankful for the financial support the German Federal Ministry of Education and Research (BMBF) provided under the auspices of the West African Science Service Centre for Climate Change and Adapted Land Use's (WASCAL) project International Master Program in Energy and Green Hydrogen.

My gratitude goes to the Rector of the University Abdou Moumouni Prof. Mamadou Saidou, to the President of the University Felix Houphouet Boigny, Prof. Ballo Zié, to the Director of GSP of Niger Prof. Rabbani Adamou at Abdou Moumouni University, to the Director Prof. Kouassi Edouard of GSP Cote d'Ivoire and my supervisor and Coordinator of the H2 Program at the GSP Dr FASSINOU Wanignon Ferdinand, to the Scientific Coordinator Prof. Soro for their tireless efforts in ensuring a conducive learning environment.

I am grateful to the Rector of the RWTH Aachen University Prof. Ulrich Rüdiger, to my supervisor and Director of the ''Institut für Eisenhüttenkunde''(IEHK) in Germany, where I had the opportunity to undertake my internship, Prof. Dr.-Ing. Ulrich Krupp as well as my co-supervisor Nima Babaei for their continuous invaluable support and mentorship throughout my research, for their valuable insights and contributions to my academic growth and for providing me with an enriching experience and constructive feedback during my internship.

My thanks also go to the members of the jury, the esteemed president Prof. Kouadio Yves and Dr. Tillous Eric the examiner from the University Felix Houphouet Boigny for their thorough assessment of this thesis.

And last but not least, to the entire team of Niger, Cote d'Ivoire, and Germany involved in the four training semesters, for their collective effort in ensuring a successful academic journey.

Their unwavering support, encouragement, and guidance have been pivotal in shaping my academic and professional growth. I am truly grateful for the opportunities they have provided me, and I look forward to making a positive impact in my field of study.

ABSTRACT (ENGLISH)

In the context of the climate crisis, new solutions and approaches such as a green hydrogen economy are proposed. The achieve such a vision, several points have to be addressed among which is the reliability of hydrogen storage and transport infrastructures. This research investigates the susceptibility of steel, especially the complex phased steel when exposed to hydrogen. In this study, hydrogen effects on steel are described as well as techniques to assess these impacts. The methodology employed in this study is focused on thermal desorption spectroscopy to assess the impact of surrounding conditions on the quantity of hydrogen that penetrates the studied material. The data for this research was collected in the laboratory and using software provided by the IEHK Institute at RWTH Aachen University in Germany. The main findings of this research reveal that current density directly linked to the hydrogen concentration, the exposure time, the pressure, and the temperature are important factors that influence the quantity of absorbed hydrogen in metallic structures. Our analysis demonstrates that an increase in these parameters leads to an increase in hydrogen absorption. Interpreting the results, it becomes evident that considerations about the acceptable level of hydrogen absorbed by a material in real-life applications such as in deep ocean water or under rainfall conditions have to be studied and clearly defined. In light of the existing literature, our results align with previous studies, corroborating the significance of the assessment of hydrogen's impact on metals and reinforcing the validity of our findings. In conclusion, this research contributes to the growing body of knowledge surrounding the implementation of a green hydrogen economy in the context of the climate crisis. Our research offers valuable contributions to the understanding of hydrogen-material interactions and their implications for the development of reliable and safe hydrogen storage and transport infrastructures in the pursuit of sustainable energy solutions amid the climate crisis.

Keywords: Hydrogen storage and transport, complex phased steel, hydrogen effects on steel, thermal desorption spectroscopy.

ABSTRACT (FRENCH)

Dans le contexte de la crise climatique, de nouvelles solutions et approches telles qu'une économie de l'hydrogène vert sont proposées. Pour atteindre ces objectifs, plusieurs points doivent être abordés, dont la fiabilité des infrastructures de stockage et de transport de l'hydrogène. Cette recherche étudie la susceptibilité de l'acier, en particulier de l'acier à phases complexes, lorsqu'il est exposé à l'hydrogène. Dans cette étude, les effets de l'hydrogène sur l'acier sont décrits, ainsi que les techniques permettant d'évaluer ces impacts. La méthodologie utilisée dans cette étude est axée sur la spectroscopie de désorption thermique pour évaluer l'impact des conditions environnantes sur la quantité d'hydrogène pénétrant le matériau étudié. Les données de cette recherche ont été collectées en laboratoire et à l'aide de logiciels fournis par l'Institut IEHK de l'Université RWTH Aachen en Allemagne. Les principales conclusions de cette recherche révèlent que la densité de courant, directement liée à la concentration d'hydrogène, au temps d'exposition, à la pression et à la température, sont des facteurs importants influençant la quantité d'hydrogène absorbé dans les structures métalliques. Notre analyse démontre qu'une augmentation de ces paramètres entraîne une augmentation de l'absorption d'hydrogène. En interprétant les résultats, il devient évident que des considérations concernant le niveau acceptable d'hydrogène absorbé par un matériau dans des applications réelles, telles que dans l'eau profonde de l'océan ou sous des conditions de pluie, doivent être étudiées et clairement définies. À la lumière de la littérature existante, nos résultats rejoignent des études antérieures, corroborant l'importance de l'évaluation de l'impact de l'hydrogène sur les métaux et renforçant la validité de nos conclusions. En conclusion, cette recherche contribue à la croissance des connaissances entourant la mise en œuvre d'une économie de l'hydrogène vert dans le contexte de la crise climatique. Notre recherche apporte des contributions importantes à la compréhension des interactions entre l'hydrogène et les matériaux, ainsi que leurs implications pour le développement d'infrastructures de stockage et de transport de l'hydrogène fiables et sécurisées dans la poursuite de solutions énergétiques durables face à la crise climatique.

Mots-clés : Stockage et transport de l'hydrogène, acier à phases complexes, effets de l'hydrogène sur l'acier, spectroscopie de désorption thermique.

TABLE OF CONTENTS

LIST OF ABBREVIATIONS AND ACRONYMS

AIDE. : Adsorption-induced dislocation emission

CP.: Complex Phase

HE.: Hydrogen Embrittlement

HEDE. : Hydrogen-enhanced Decohesion

HELP. Hydrogen Enhanced Localised Plasticity

IEHK. : Institut für Eisenhüttenkunde

TDS.: thermal desorption spectroscopy

WASCAL. : West African Science Service Centre for Climate Change and Adapted Land Use

LISTS OF FIGURES

LIST OF TABLES

GENERAL INTRODUCTION

GENERAL INTRODUCTION

Hydrogen as an energy carrier is a concept that is gathering more and more attention. It is indeed a promising candidate in the path to decarbonising the global energy sector in this context of climate change. Although hydrogen has been known and manipulated for a long time, the implementation of a heavy hydrogen economy gives rise to new challenges among which the technological aspect of storage and transportation. Being very reactive, the molecule tends to attack its steel-made vessels. Research is still ongoing to understand and cope with this important problem.

This work's objective is to investigate the hydrogen absorption and desorption by high-strength steels with a focus on complex phase (CP) steel. It aims to relate naturally occurring conditions that materials can be exposed to, to experimental setup ones. To achieve this objective, this work will go through three main points constituting the different chapters.

In the first part which is the bibliographical review, the study will give the context and look over the current state of hydrogen storage and transport technologies then provide a comprehensive review of existing literature on hydrogen effects on steels, identifying gaps and limitations in the current understanding.

The ‘’Materials and methods’’, as well as all the processes used during the experimentations will be then described. All the assumptions made and the parameters considered during the different experiments will be clearly defined and described here. We will examine CP steel and its performance in hydrogen-rich environments under different conditions through various experiments.

The following chapter ‘’Results and Analysis’’ will describe all the observations and founding from the experimentations. Then we will analyse the results, compare them to those obtained by other researchers and draw conclusions from our observations.

CHAPTER I:
BIBLIOGRAPHICAL REVIEW

CHAPTER I: BIBLIOGRAPHICAL REVIEW

INTRODUCTION

In this chapter, we will start with a short background to contextualize the study and investigate the current state of the art of hydrogen storage and transport technologies. Then, we will provide an overview of the existing literature related to the challenges of materials characterisation and design for hydrogen storage and transport.

1. BACKGROUND AND CONTEXT OF THE STUDY

1.1. Climate Crisis

Our world has, today, reached a level of development never seen before. Advancements in technology, science, and medicine have led to an exponential increase in the population. Along with the increase of the population, comes the increase of needs. Energy, food, and water demands are enormous. Since 1850, the growth rate of the world's primary energy consumption has been extremely consistent (2.4% per year 70.08%) and does not appear to be slowing down[1].

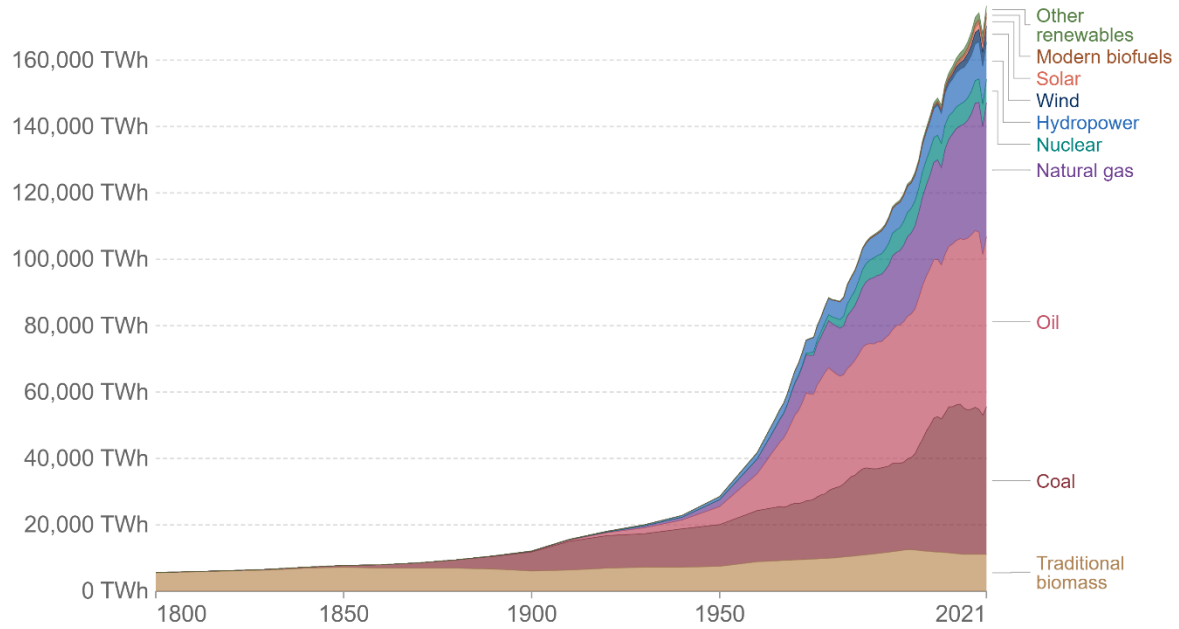

Figure 1: Global primary energy consumption by source[2].

To face this enormous energy demand, the most used method was and is still fossil fuels. There is no doubt that the use of fossil fuels has significantly advanced technology recently, however, the problem is the rise in pollution, which reached a point where Earth could no

longer sustain itself without suffering the repercussions. Currently, these detrimental impacts may be seen in many different ways, with climate change being the most prominent one[3].

Fossil fuel combustion produces greenhouse gas emissions which, once in the atmosphere, trap heat from the sun and increase temperatures. Carbon dioxide and methane are the primary greenhouse gases responsible for climate change. These are produced, for instance, while burning coal or gasoline to heat a building. As the issue of climate change is threatening our society, measures are to be taken.

1.2. A hydrogen-based economy and challenges

In order to face the climate change issue, all over the world, the energy transition, which is the use of renewable energy such as photovoltaics, wind, geothermal, hydropower, and biomass instead of fossil sources, is being promoted. However, renewable energies generally suffer a huge drawback, the intermittency of their sources. They depend for their energy production, on the seasons and the weather, therefore they cannot be 100% reliable when it comes to applications such as industry.

As a complement to the use of renewable energies, hydrogen as an energy vector is getting more and more momentum. Hydrogen is already produced and used for many applications. It is extensively employed in refineries for hydrocracking and desulfurization, in agriculture for fertilizer production, in the manufacturing of ammonia and methanol, in the processing of food, and in other applications[4]. The characteristic of the molecule that is currently capturing global attention is its capacity to be generated and utilized in an environmentally friendly manner, hence the term “green hydrogen”.

In periods of abundance like windy and sunny days, green hydrogen is produced from wind turbines and photovoltaic panels respectively, then stored for a more or less long period in small or high quantities before being used when and where the need arises. Hydrogen, when used, only produces water as a by-product. This makes it a really interesting tool to step out of the carbon economy.

The solution is therefore the implementation of a hydrogen-based economy. However, this is challenged by storage and transportation issues. Although the hydrogen molecule is very light and energetic in terms of mass, the energy density per volume is very low. In comparison to fossil fuels, hydrogen has a poor energy density by volume (9.9MJ/m^3 LHV), which could necessitate extraordinarily large storage tanks. To prevent it, storing enough hydrogen must have at least one of the three features listed below high storage pressure, low storage temperature, or employing materials that can absorb hydrogen molecules. When it comes to

high-pressure storage, four different pressure containers can be used to store hydrogen: Type I: Fully metallic pressure vessels, type II: Steel pressure vessel with a glass fibre composite overwrap, type III: Full composite wrap with metal liner, type IV: Fully composite and a full composite, linerless pressure vessel (also known as Type V) exists and is in the pre-commercial stage [4].

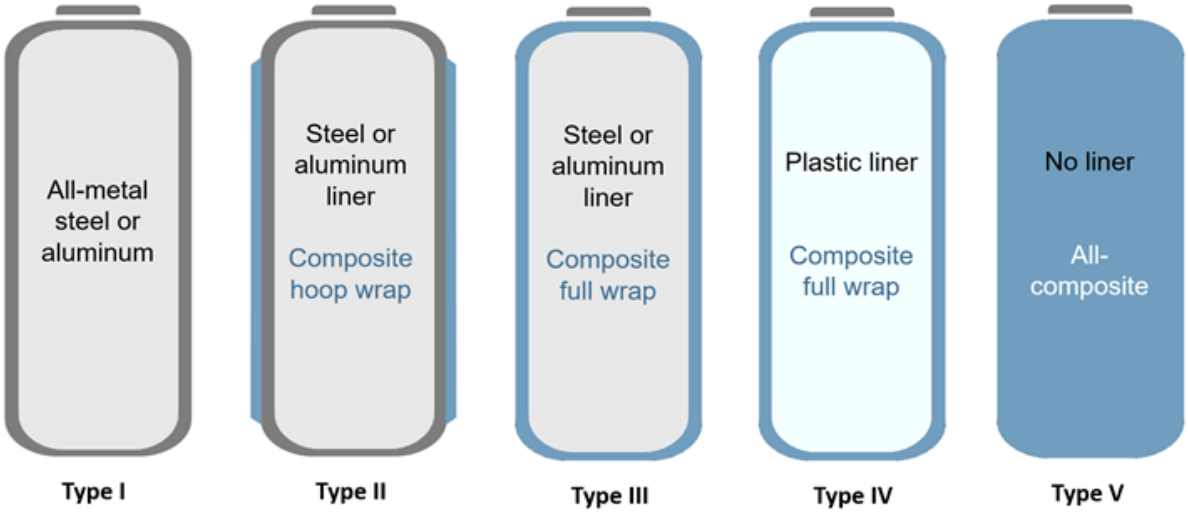

Figure 2: Different types of pressure vessels for hydrogen storage[5].

Due to the characteristics of the hydrogen molecule, hydrogen storage solutions are a crucial component of hydrogen systems. This is particularly important to remember while using big projects and processes [3]. The challenge lies in the fact that hydrogen is a very reactive element and at high pressure, it tends to attack the vessels that contain it, resulting in risks and failures. Atomic hydrogen-assisted cracking or “hydrogen embrittlement” (HE) which is the fatigue of material due to the attack of hydrogen, is a major challenge. Failures due to this phenomenon cause a lot of damage and are extremely costly. Now that a hydrogen-based economy is being investigated it is more urgent than ever to address this challenge as soon as possible. It is therefore very important to explore new hydrogen-resistant materials to ensure the reliability of hydrogen storage and transportation as reliability will be a determining factor in the acceptance of the new hydrogen economy by the consumers.

2. FUNDAMENTALS OF HYDROGEN EMBRITTLEMENT

2.1. Definition and Significance of Hydrogen Embrittlement

HE is referred to as the process by which the introduction of a hydrogen atom when working in a hydrogen environment can dramatically lower a material's strength. The material simultaneously loses ductility and becomes brittle [6].

HE is a widely known phenomenon in high-strength materials. The development of subcritical cracks, the beginning of fractures, and catastrophic failure with the ensuing loss of mechanical qualities like ductility, toughness, and strength are all caused by HE. During electrochemical reactions and high-pressure gaseous hydrogen environments, this hydrogen is induced in the material [6].

Three conditions combine to result in HE, a sensitive material subjected to a mechanical load in the presence of hydrogen. Some materials are more susceptible to HE than others: high-strength steels, titanium, and aluminium alloys[6].

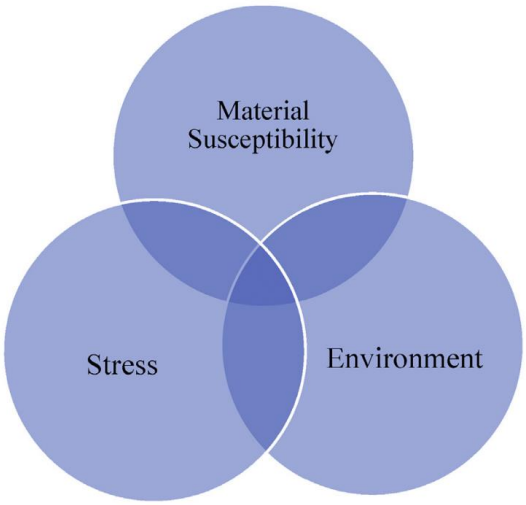

Figure 3: Factors responsible for HE[6].

There are two types of HE known. The first is the environmental HE where the hydrogen source is the metal's external environment. In a hydrogen-rich environment, the material is attacked through a corrosion process. The second type is internal HE where hydrogen is internal and originates from the manufacturing during cleaning or plating processes[7].

Upon absorption or internal diffusion of hydrogen, the metal becomes brittle or starts fracturing. HE is a complex phenomenon that is still not completely understood. Some mechanisms by which it occurs have been theorised based on experimental observations:

internal pressure theory[8], Hydrogen enhanced Decohesion (HEDE), Hydrogen Enhanced Localised Plasticity (HELP), adsorption-induced dislocation emission (AIDE) [6].

2.2. Mechanisms of Hydrogen Embrittlement

2.2.1. Internal pressure theory

The first documented faults in steel caused by hydrogen are internal fissures. Bright facets indicated the presence of a high-pressure molecular hydrogen precipitate. The sites of this precipitation were thought to represent "inter-block disjunctions" in the crystals responsible for the localised cleavage and rupture. During the manufacture of steel, atmospheric moisture serves as the main source of hydrogen[8]. High hydrogen concentrations cause pressure inside the metal as absorbed hydrogen species combine to produce hydrogen molecules (H_2) in voids. This pressure can rise to a point where fractures or blisters appear on the specimen surface, both of which are referred to as hydrogen-induced cracking (HIC) and hydrogen-induced blistering, respectively. Tensile strength and ductility and other material parameters are highly affected by these phenomena.

2.2.2. Hydrogen-enhanced decohesion mechanism (HEDE)

Troiano initially presented this method in 1959. It is based on the permeation of hydrogen atoms, which reduces the cohesive strength of a material at the crack tip area. Due to the hydrogen electron entering the lattice cell of the iron, the interatomic bond strength between the atoms decreases. When the critical crack tip opening displacement is attained, decohesion occurs. When a material has hydrogen atoms accessible everywhere around it and stress is applied, the hydrogen atom diffuses within the material, reducing the cohesive or interatomic strength of the material at the crack tip and causing a cleavage-like fracture. Surface energy is decreased along with a material's cohesive strength, which lowers the fracture stress and lowers the allowed value of fracture. The sole restriction on using this model is determining the cohesive force [6].

2.2.3. Hydrogen-enhanced localised plasticity (HELP)

This theory is highly supported and was initially introduced in 1972. According to this idea, hydrogen that has gathered close to the crack's tip reduces the barrier to dislocation motion, increasing its mobility and causing dislocations to act as carriers of plastic deformation in a metal lattice[6]. Thermodynamic simulations and microscopic observations support this

process. The hydrogen-enhanced localised plasticity mechanism is based on observations that the presence of hydrogen in a solid solution lowers the barriers to dislocation motion at a range of temperatures and strain rates, increasing the deformation in a localised region near the fracture surface. Instead of embrittlement, the fracture is a highly confined plastic failure process. This paradoxical phenomenon, which is verified by microscopic studies, states that the development of substantial localised plasticity limits macroscopic ductility [9].

2.2.4. Adsorption-induced dislocation emission (AIDE)

This system combines the best aspects of HEDE and HELP. Hydrogen atoms from the solute are adsorbed at the surface in areas where there is a concentration of stress, such as fracture tips. According to the HEDE mechanism, hydrogen adsorption at the crack tip causes the material's interatomic bonds or cohesive strength to diminish. It also makes it easier for dislocations to be injected from the crack tip, which leads to crack propagation via slip and the creation of micro voids according to the HELP mechanism. Decohesion and dislocation emission at the fracture tip are the causes of crack nucleation and growth in this process. The combined effects of slip at the crack tip and micro-void coalescence (MVC) led to crack development and simultaneous fracture. a significant quantity of hydrogen adsorbed on the surface. Fe, Ni, and Ti have been found to have significant amounts of adsorbed hydrogen on their surfaces, supporting the AIDE process. [6]

3. MEASUREMENT METHODS FOR HYDROGEN EMBRITTLEMENT

3.1. Electrochemical Hydrogen Charging

The examination of the amount of hydrogen present in the subject is crucial when analysing the impact hydrogen has on a material. To do this, we resort to ‘’Hydrogen charging”. A sample is typically charged with hydrogen either by electrochemical cathodic charging or with high-pressure hydrogen gas. These charging methods result in hydrogen spreading into the material, which degrades its characteristics and results in HE[6].

Electrochemical hydrogen charging, which interests us here, is an experimental method whereby hydrogen is carefully injected into metallic samples. To perform electrochemical hydrogen charging experiments, a metallic sample is carefully selected and prepared. It must be an accurate representation of the materials utilised in the targeted application. A compact disc or sheet with predetermined dimensions, such as a circular disc with a diameter of a few centimetres or a rectangular sheet with predetermined length and width, is a typical form for

the sample. Since the metal-electrolyte interface is where the electrochemical reactions take place, the sample's surface area is thus a crucial factor. As a result, the sample's dimensions must be precisely known and well-defined.

An electrical potential is applied between the metal sample and a reference electrode after submerging it in an electrolyte solution, usually, an acidic solution containing hydrogen ions. The electrolyte to use is determined by the particular requirements of the experiment and the material under study. Sulfuric acid (H_2SO_4) and hydrochloric acid (HCl) are two electrolytes that are frequently used. As the electrochemical reaction requires hydrogen ions (H^+), the acidic solution is crucial. Hydrogen atoms or ions can permeate into the metal lattice as a result of the electrochemical process.

The sample is connected to the negative pole of the generator in order to attract positively charged hydrogen ions H^+ and the second electrode usually in platinum is connected to the negative pole. The platinum is commonly used as an electrode because of its high conductivity and its inertness. If the connexions were made the other way round, with the sample connected to the positive pole and the platinum to the negative, the sample would attract oxygen ions and undergo corrosion.

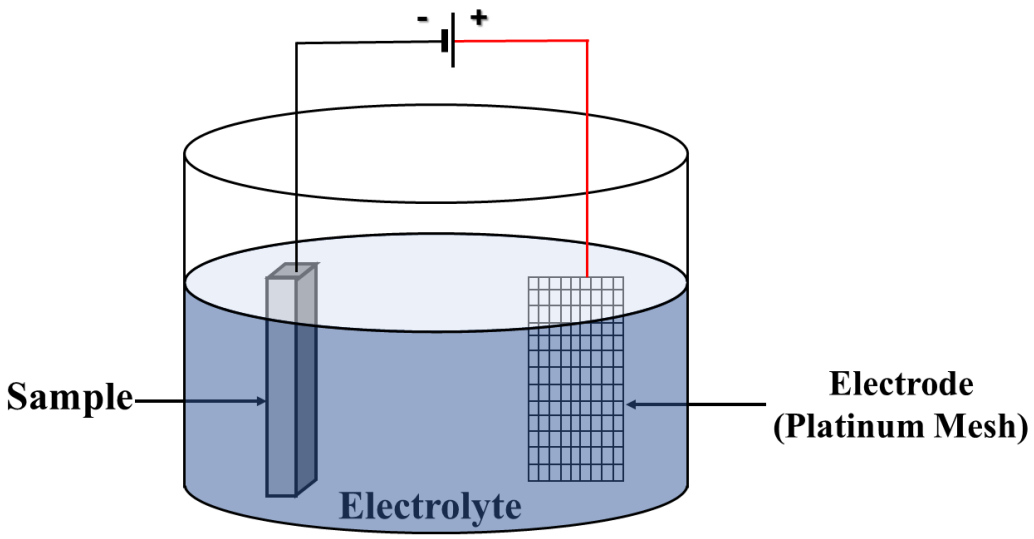

Figure 4: Experimental setup for electrochemical hydrogen charging.

After the electrochemical cell is set up, an external electrical potential is provided between the reference electrode and the metallic sample. At the metal-electrolyte interface, this potential generates an electric field. At the metal-electrolyte interface, electrochemical processes take place. At the sample surface, hydrogen gas (H_2) changes, and the metal lattice produces

hydrogen ions (H^+). The produced hydrogen ions diffuse into the metal, causing the sample to absorb hydrogen.

The metallic sample is carefully taken out of the electrochemical cell and ready for hydrogen measurement when the charging procedure is finished. The amount of hydrogen absorbed by the sample can be measured using a variety of methods, including thermal desorption spectroscopy (TDS) and gas chromatography.

Electrochemical hydrogen charging and high-pressure hydrogen charging are two common methods for introducing hydrogen into materials for laboratory studies used to mimic real-life conditions. In nature, various sources of hydrogen are available to charge exposed materials, water vapour from the ambient, furnace charge components, slag compounds, alloy additives, and refractory linings[10]. In order to investigate HE and create materials that can tolerate hydrogen exposure, it is essential to comprehend the sources of hydrogen and how it can interact with materials in practical settings. Using techniques like electrochemical hydrogen charging and high-pressure hydrogen charging in the lab, researchers can simulate and analyse the effects of hydrogen on materials, which aids in the creation of safer and more resilient materials for hydrogen-related applications.

3.2. Slow Strain Rate Test

The slow strain rate test consists essentially of a tensile stress test on a typical smooth tensile specimen that is steadily lengthened till fracture while maintaining a constant strain rate[11]. The slow strain rate test is used to measure very important properties of materials. Stress-strain curves, that are obtained from tensile tests give information about the Ultimate Tensile Strength, Yield strength, ductility, toughness, resilience and the Young Modulus.

The Ultimate Tensile Strength is the maximum stress that is reached during the test. The Yield strength is the stress beyond which the material starts to deform plastically. It represents the limitation in elastic applications. Ductility is the degree to which the material can withstand plastic deformation before fracture. Materials with high ductility are said to be ductile and materials with low ductility are said brittle. The toughness is a measurement of a material's capacity to absorb energy up until fracture. Resilience is a material's capacity to absorb energy while undergoing plastic deformation. Young’s Modulus is the ratio between the stress and the strain in the linear region of the stress-strain curve which represents the elastic deformation. It can be measured as the gradient of the slope of the linear region. It is a measure of how stiff the material is.

According to HOOKE’s law:

$$\sigma = E.\varepsilon$$

σ: stress (psi/Pa), ε: strain($\frac{\Delta l}{l}$), E: Young's modulus (psi/Pa)

The slow strain rate test is also used to assess the impact HE has on these mechanical properties of materials.

3.3. Thermal Desorption Spectroscopy (TDS)

Also called temperature-programmed desorption, TDS is a very popular method for analysing hydrogen absorption as well as many other elements' absorption into metals. As the absorbed hydrogen has a significant impact on the properties of a material and the initiation of, HE, it is important to know how much a material is susceptible to hydrogen absorption. This can be qualified and quantified using TDS.

By using a regulated and constrained amount of heating, the TDS method can measure the amount of absorbed hydrogen. Steel has traps that are responsible for hydrogen accumulation. Hydrogen is released when a certain amount of absorbed energy, which is equivalent to the desorption activation energy, is reached when heat is applied to steel. Hydrogen absorbs the thermal energy. The temperature at which hydrogen atoms are released is hence the desorption temperature[6].

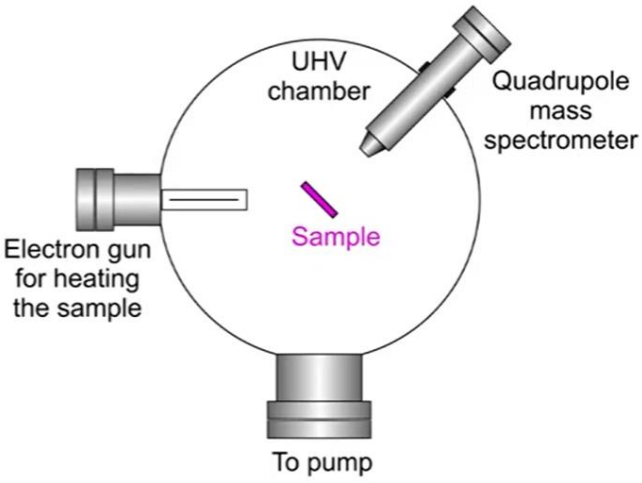

Figure 5: TDS setup

The experimental setup for TDS is an Ultra High Vacuum chamber (UHV) in which a sample that has undergone hydrogen charging is placed. The UHV is necessary in order to avoid any parasite element in the chamber. The electron gun is used to heat at a controlled rate the sample. The absorbed elements upon absorption of thermal energy diffuse out of the sample. Depending on the temperature, the nature and the quantity of the element that comes

out of a sample can significantly vary. The quadrupole mass spectrometer is then used to detect a specific element or molecule that is desorbing from the sample by adjusting to its mass. Therefore, it is possible to get the amount of desorbed element as a function of the temperature or a function of time.

3.4.Hydrogen Permeation Test

Hydrogen permeation testing is used to determine how much hydrogen is diffusible in steel. The electrochemical permeation test is one of the techniques most frequently used to assess hydrogen diffusion in metals. The flux of hydrogen atoms registered in the oxidation cell might be fitted to obtain apparent diffusivities. The magnitude of this coefficient has a decisive influence on the kinetics of fracture or fatigue phenomena assisted by hydrogen and depends largely on hydrogen retention in microstructural traps [12].

Two cells must be separated using the tested metallic sheet for this procedure. In one cell, processes involving adsorption and absorption occur on the specimen's entrance surface while hydrogen is created through a cathodic reduction. Hydrogen output flow is recorded in the oxidation cell after penetrating. It has been shown how crystal flaws slow penetration, and the influence of the microstructure has been thoroughly examined. Permeation through a sample containing a certain number of flaws, such as dislocations, grain boundaries, inclusions, etc., exhibits a lower diffusivity than an ideal lattice-free of flaws[12]. This effect, known as hydrogen trapping, is crucial for predicting and reducing hydrogen buildup close to a crack tip.

4. HIGH STRENGTH STEEL

4.1.History, definitions and fundamentals

High-strength steel is a type of steel that, as compared to traditional or low-carbon steels, has improved mechanical qualities, especially in terms of strength and hardness. These steels are designed to have higher yield strengths, tensile strengths, and deformation resistance, enabling them to tolerate larger loads and stresses. Several approaches, including alloying components, heat treatment procedures, and controlled cooling techniques during manufacture, are used to boost the strength. High-strength steels are frequently utilized in sectors like manufacturing, aerospace, automotive, and construction where performance and efficiency are improved by reducing weight and increasing strength.

As for history, the use of steel in automobile manufacturing began in the late 19th century. The automotive industry predominantly relied on low-carbon steels for over 100 years, which

provided the desired balance of strength, cost, and formability. The shift towards higher-strength steels began in the 1970s to improve fuel economy and meet regulatory requirements. Initially, the industry faced challenges in handling high-strength low alloy steels due to their limited ductility and inconsistent manufacturing processes[13].

Early attempts at using high-strength steels faced difficulties, including forming cracks and spring back. Lack of understanding and inconsistent steel production processes hindered their successful implementation. It took around 20 years for the industry to learn valuable lessons and effectively incorporate high-strength steel into vehicle designs, delaying the weight savings and structural improvements they could offer.

This table summarizes the different types of hard-strength steels existing in the automotive industry:

Table 1: Different types of hard-strength steels existing in the automotive industry[13]

Low-carbon and conventional high-strength steels
Low carbon steels (LC) Solid solution strengthened (SSS) Bake hardenable (BH) High strength low alloy (HSLA)
First-generation advanced high-strength steels
Dual-phase (DP)—ferrite/martensite High hole expansion (HHE)—ferrite/bainite Stretch flangeable (SF) Transformation-induced plasticity (TRIP) Complex phase (CP) Fully martensitic (MS) Boron heat-treatable steels
Second-generation advanced high-strength steels Twinning-induced
Twinning-induced plasticity (TWIP) Lightweight steels with induced plasticity (L-IP)

4.2.CP steel

4.2.1. Introduction:

CP steel is an advanced high-strength steel (AHSS) that contains martensite, pearlite and retained austenite. The distribution of hard martensite islands within a matrix of soft ferrite and bainite gives the CP steel its strength. These phases work together to increase strength and ductility, which makes CP steel appropriate for a variety of demanding applications.

4.2.2. Manufacturing of CP steel:

To achieve the necessary microstructure and mechanical properties during the production of CP steel, the cooling process must be carefully managed after hot rolling. The microstructure must undergo several heat treatments to become a complex combination of ferrite, bainite, and small martensite islands. The typical processes that CP Steel goes through are as follows:

Hot rolling is the first stage in the manufacture of complex-phase steel. In hot rolling, the thickness of the steel is reduced by first heating it to a high temperature and then passing it through several rolling mills. This procedure ensures a more homogeneous microstructure by improving the grain structure and aligning the crystallographic orientations.

The steel is then heated to a temperature where it transforms into an austenitic microstructure. Austenite is a face-centred cubic (FCC) crystal structure that forms at elevated temperatures. This stage is crucial for ensuring uniformity in the subsequent cooling process. The following step is quenching, a controlled cooling procedure, which has a substantial impact on the resultant microstructure. The production of hard and brittle martensite as a result of the high cooling rate during quenching adds to the material's strength. However, too much martensite can reduce a material's toughness and formability, thus careful cooling rate management is required.

After quenching, the steel is heated to a range of temperatures known as the intercritical area for intercritical annealing. Within this range, martensite partially recrystallizes and changes into a mixture of bainite and retained austenite. The process of creating CP steel entails quenching the material one more time after another quick cooling. The residual austenite is successfully transformed into martensite by quick cooling, creating the CP steel with its distinctive microstructure.

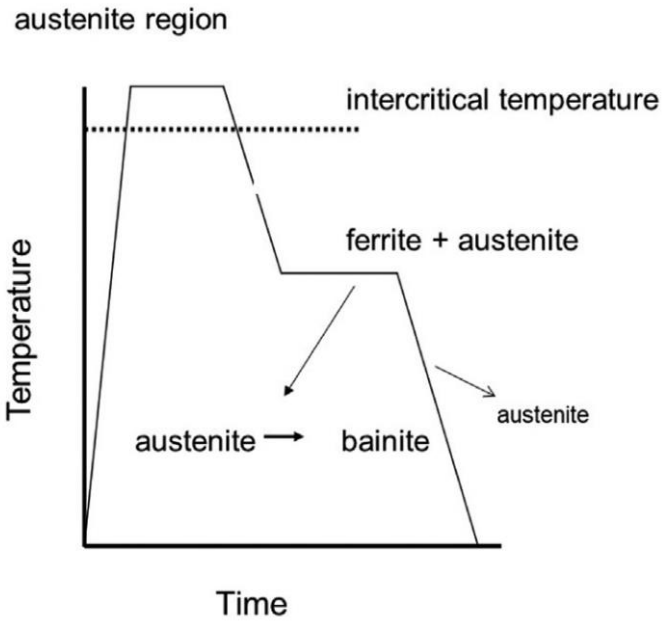

Figure 6: Typical cooling curve of CP steels[13].

4.2.3. Properties of CP steel

A fine ferrite microstructure and a large volume proportion of hard phases are all present in complex-phase steels. These steels' precipitation hardening is done by using niobium, titanium, and/or vanadium in addition to the usual alloying components used in dual-phase and TRIP steels. The result is that the CP steels have very high strength and are being used increasingly frequently to achieve strengths of 800 MPa and higher. The complex-phase steels can achieve higher strengths with lower alloy contents, which enhances weldability at a lower cost, even though their formability does not come close to that of TRIP steels[13].

Complex-phase steel is a unique material in the engineering community thanks to its advantageous mix of mechanical attributes. It enables lighter components without sacrificing performance because it has a higher tensile strength than ordinary steel. It is amazing that despite having great strength, the material still has good formability and drawability, allowing for the creation of complicated shapes and deep-drawn components. Its outstanding toughness is further enhanced by the presence of ferrite and bainite, which guarantees resistance to crack propagation and makes it the perfect option for crucial vehicle safety components. Last but not least, CP steel features martensite, which allows for work-hardening behaviour and adds strength during forming processes, making it a flexible material for a variety of applications.

4.2.4. Applications:

The automobile industry has benefited greatly from the extensive use of CP steel in a variety of sectors. It has become a crucial material for structural and safety components in this field. Automotive Body-in-White, where CP steel is used to make vehicle body structures, is one typical use[13].

Furthermore, CP steel is an essential component for safety elements including door impact beams, roof reinforcements, and front-end structures due to its excellent energy-absorption properties. Beyond safety, the lightweight and high-strength qualities of the steel enhance chassis parts including suspension and structural elements, greatly enhancing total vehicle performance and fuel efficiency. Beyond the automobile industry, CP steel is used in a variety of other industrial fields.

CONCLUSION

In conclusion, the study has examined the significant aspects of HE and its importance with regard to the climate change problem and the growth of a hydrogen-based economy. We have investigated the basic mechanics of HE and discussed its potential negative impacts on high-strength steels.

The investigation of HE mechanisms as well as its measurement methods has highlighted the significance of precise and trustworthy methods for determining the susceptibility of materials to this process. These techniques are essential for guaranteeing the security and endurance of high-strength steel constructions.

Through laboratory tests with diverse initial conditions and parameters, this study intends to examine the behaviour of high-strength steels in hydrogen-rich environments. CP steels will be the main focus of the results discussion.

This work helps the larger efforts in tackling the climate problem and building a more sustainable future by offering thorough insights into the impact of hydrogen on the characteristics and nature of high-strength steel.

CHAPTER II:

MATERIALS AND METHODS

CHAPTER II: MATERIALS AND METHODS

INTRODUCTION

This chapter focuses on describing how the study of the impact of hydrogen on our material is done. By conducting several experiments on a chosen sample (CP1180), we aim to understand the impact hydrogen can have on materials. The chapter will provide detailed information about the material used and then describe the experimental setups, the steps and the methodology employed in our research.

1. MATERIAL: CP1180

The main focus of this work will be the CP 1180 steel. It is a type of CP steel with high strength and good formability. As with most of CP steels, the microstructure of CP 1180 steel consists of a ferrite/bainite matrix with pearlite and retained austenite, and small quantities of martensite. The microstructure is refined by the retarded recrystallization or precipitation of microalloying elements such as Nb or Ti. CP 1180 steel has a high yield strength of over 850 MPa and a tensile strength of over 1180 MPa.

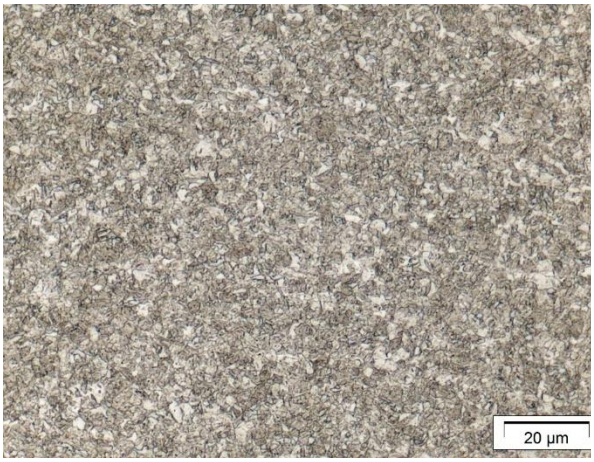

Figure 7: CP 1180 1000x

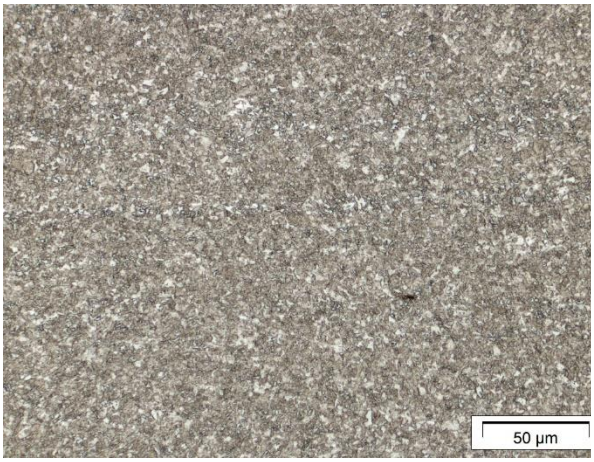

Figure 8: CP 1180 500x

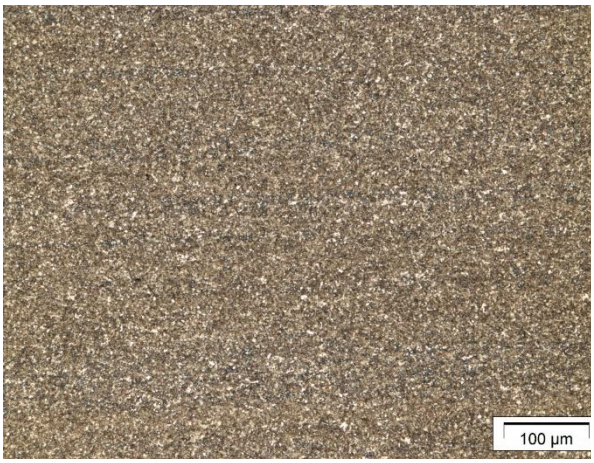

Figure 9: CP 1180 200x

Figure 10: CP 1180 100x

CP steels like CP1180 steel are renowned for their high strength and exceptional formability. However, they become embrittled as a result of hydrogen exposure and suffer considerable reductions in tensile strength, ductility, and fracture toughness. Consequently, the environment and the material's susceptibility to hydrogen must be taken into account when designing goods that will be exposed to hydrogen, thus, the importance of studying the impact of that exposure on the metal.

In this work, CP 1180 steel will be tested through SSRT and TDS tests to compare the effects of different conditions on our material.

2. SLOW STRAIN RATE TEST:

2.1. Description of the experiment:

As mentioned previously the slow strain rate test consists in elongating a metallic sample and studying the evolution of its properties. In our case, we did the SSRT experiment simultaneously with the hydrogen charging of the sample in different conditions.

The experiment takes place in a controlled environment with a laboratory supervisor and the processes are as follows:

The preparation of the sample: The material is chosen and the dimensions are measured precisely.

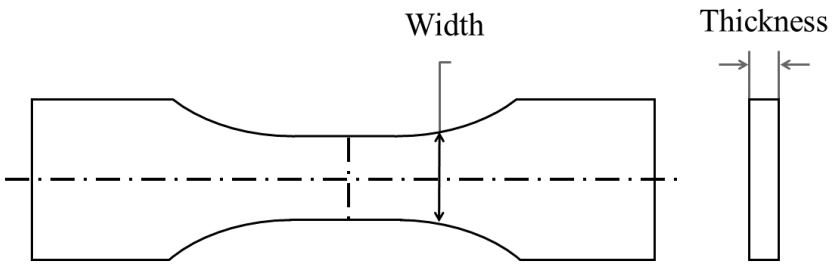

Figure 11: Dimensions and geometry of the sample

The sample is washed with distilled water and then with ethanol to remove any external element from the surface. A PTFE tape is then used to cover the tip surfaces of the sample as shown big the figure below.

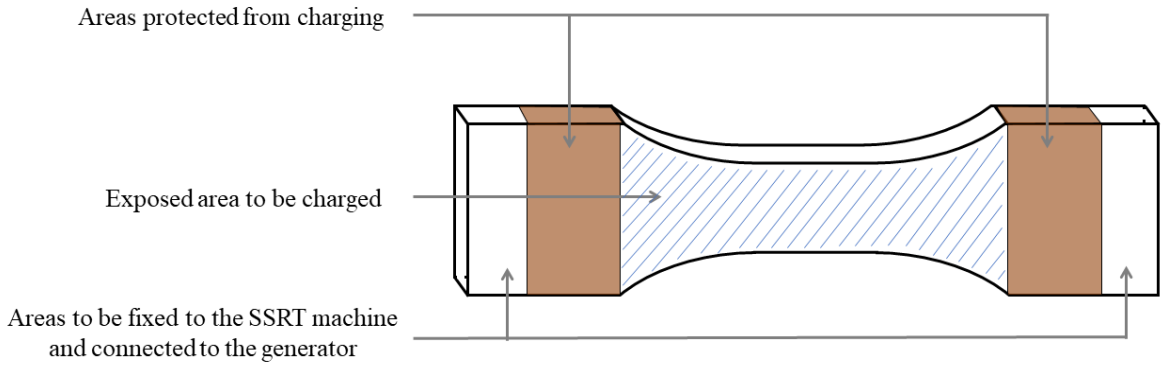

Figure 12: Exposed area of the sample that will be in contact with the acid solution and undergo the hydrogen charging

That action is performed because not all the surface of the sample is supposed to undergo hydrogen charging. The remaining exposed face is measured as well and is very important for the charging process.

The sample is then placed in the SSRT machine shown in Figure. It is controlled numerically by the software C-Lab viewer developed at the IEHK Institute.

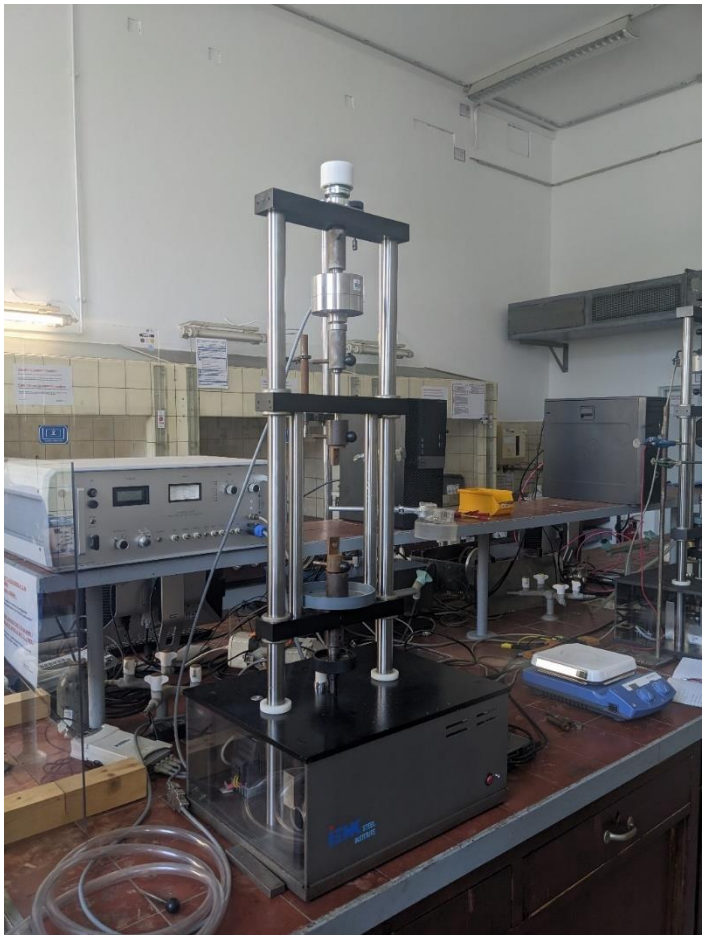

Figure 13: Slow Strain Rate Test machine

The parameters such as the pressure at which the test will run, the duration of the experiment and the current density of the charging are chosen. The other parameters are calculated such as the force and input in the software. The machine starts then stretching the sample readjusting slowly the value of the force. The axe of the sample is not forcingly aligned with the force; therefore, the sample is not completely tightened up, allowing it to readjust when the force is applied.

After usually one hour, the machine reaches the constant value of the force needed, and the charging starts. The objective is to charge the sample with hydrogen so it is connected to the negative pole of a generator in order to attract the hydrogen ions H^+. The positive pole is connected to an electrode made of platinum. The generator is turned on before the electrolyte is introduced. The reason is that it impedes corrosion due to the acid. The electrolyte used here is the 0.05M H_2SO_4. The formation of bubbles at the surface of the sample showing the

formation of hydrogen ions is directly observed. This setup is the hydrogen charging at constant load used for the test of our different material and it is shown by the figure below.

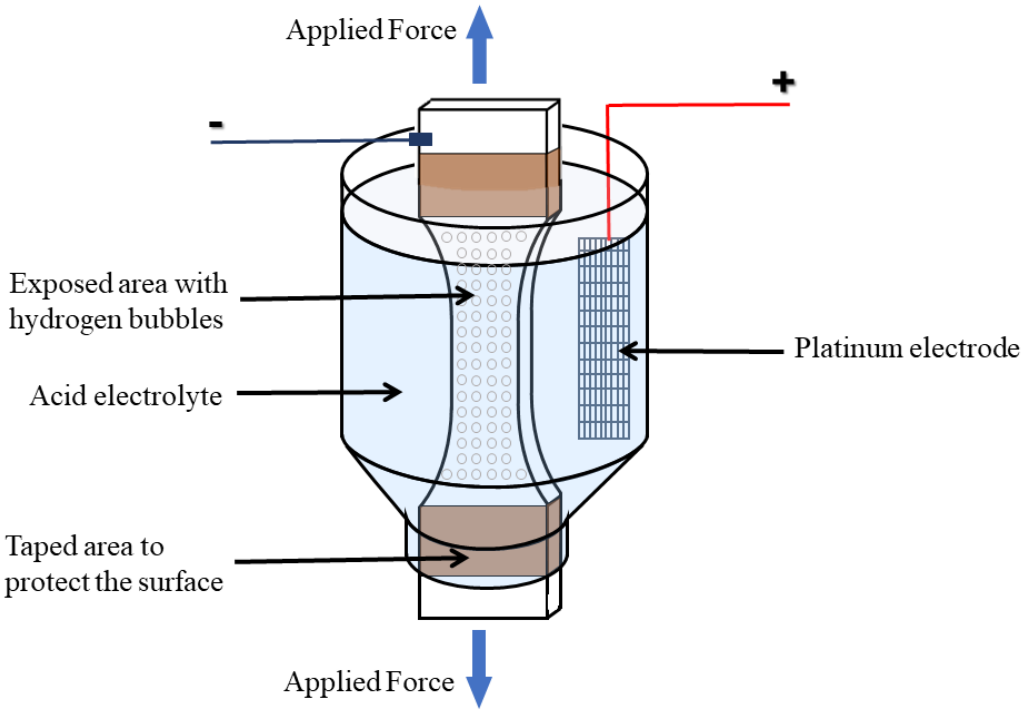

Figure 14: Setup of the sample for the SSRT

The sample, after approximately one hour of hydrogen charging at constant load, is retrieved and then cleaned thoroughly first with distilled water, and then with ethanol. The following step is to put the sample in liquid nitrogen at -196ºC. It is important to note that liquid nitrogen should only be used in well-ventilated areas otherwise it will replace the air and make the environment toxic.

The aim is to decrease the temperature of the metal enough to make it breakable. After 10min of deep in the liquid nitrogen, the sample is taken out and broken into four pieces. The two uncharged tips are removed and the charged part is broken into two pieces as well. These two will undergo TDS.

2.2. Conditions and parameters for the different experiments :

2.2.1. Conditions:

The dimensions were measured: 1.41mm for the thickness and 5.11mm for the width, with an exposed surface of A=527.74mm^2.

2.2.2. Parameters

The parameters chosen for the experimentation were:

- A pressure of P=50 MPa
- A time of T=1h
- Current density j=0.02mA/cm^2

From the pressure and the dimensions of the sample (Thickness: T and Width: W), it was possible to calculate the force that would be applied on the cross-section (S) :

$$F = P.S = P.T.W \quad \text{Eq. 1}$$

$$F = 50 \times 10^6 \times 1.41 \times 10^{-3} \times 5.11 \times 10^{-3}$$

$$\boldsymbol{F = 360N}$$

From the current density and the sample surface, we calculated the value of the current:

$$I = j.A \quad \text{Eq. 2}$$

$$I = 0.02mA/mm^2 \times 527.74$$

$$\boldsymbol{I = 0.105mA}$$

3. THERMAL DESORPTION SPECTROSCOPY:

3.1. Description:

The TDS was conducted on different samples previously charged with hydrogen in different conditions. The aim is to determine the quantity of hydrogen that was present in the samples. The results will be compared to highlight the effect of the charging current and the internal pressure on the quantity of hydrogen absorbed.

For this experiment, the sample is placed in a vacuum chamber and heated at a constant heating rate. The hydrogen inside the material will gain energy and escape. The escape hydrogen is captured by a mass spectroscometer. With this experiment, the influence of stress and time on the particle content is analysed.

3.2. Conditions and parameters:

Several experiments were conducted with various charging currents and pressures.

Experiment 1: The sample CP1180 was subjected to thermal desorption without hydrogen charging. The reason was to have a base study of the material to which the subsequent results will be compared.

The initial temperature was 21°C and the factor was 2147.8750ppm/s.

Experiment 2: The sample CP1180 was subjected to thermal desorption and charged under a charging current of 0.02mA/cm^2, a pressure of 0MPa and for 1h.

Experiment 3: The sample CP1180 was subjected to thermal desorption and charged under a charging current of 0.02mA/cm^2, a pressure of 100MPa and for 1h.

Experiment 4: The sample CP1180 was subjected to thermal desorption and charged under a charging current of 0.02mA/cm^2, a pressure of 100MPa and for 6h.

Experiment 5: The sample CP1180 was subjected to thermal desorption and charged under a charging current of 0.02mA/cm^2, a pressure of 100MPa and for 12h.

Experiment 6: The sample CP1180 was subjected to thermal desorption and charged under a charging current of 0.02mA/cm^2, a pressure of 300MPa and for 1h.

Experiment 7: The sample CP1180 was subjected to thermal desorption and charged under a charging current of 0.02mA/cm^2, a pressure of 300MPa and for 6h.

Experiment 8: The sample CP1180 was subjected to thermal desorption and charged under a charging current of 0.02mA/cm^2, a pressure of 300MPa and for 12h.

CONCLUSION:

This chapter has presented the material of our interest, the CP1180 steel. The important information about the sample such as the geometry and the dimensions was described, and then the conducted experiment. The focus has been made on the slow strain rate and the TDS. Those two experiments will provide valuable information to understand the influence of several parameters on metallic materials. With the materials and the conducted experiments thoroughly described, the analysis and interpretations can be undertaken clearly.

CHAPTER III:

RESULT AND ANALYSIS

CHAPTER III: RESULTS AND ANALYSIS

INTRODUCTION:

In this chapter, the results of the TDS experiments are presented, analysed and finally compared to existing literature.

1. THERMAL DESORPTION SPECTROSCOPY RESULTS:

1.1. Experiment 1 _ CP 1180 without charging:

The results collected are presented in a table with the temperature of the sample and the quantity of desorbed particles of hydrogen. As described in the material and methods chapter, two sample are collected to undergo the TDS but the result is really close therefore just one set of results will be chosen for the study. There were 4955 entries for the chosen sample, which is a lot so the table below just presents the general aspect of the data.

Thanks to these data the graph of the quantity of desorbed particles with respect to the temperature can be plotted.

Table 2: Results (Temperature, time, particle content) of the TDS of the CP 1180 steel without prior charging

Temperature (^{o}C)	Particle content (ppm/s)
21.00	180
21.00	180
21.00	180
. . .	. . .
538.00	175
538.00	176
538.00	176
. . .	. . .
900.00	180
900.00	180

901.00	180

The resulting graph is:

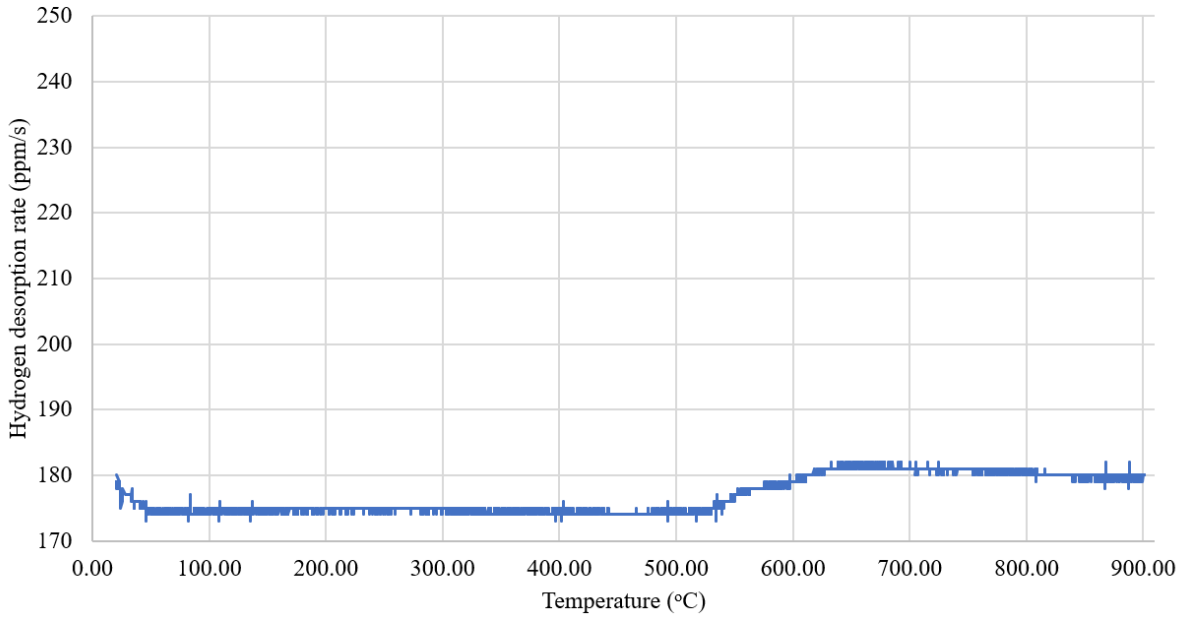

Figure 15: TDS curve of CP1180 without hydrogen charging, evolution of the quantity of desorbed hydrogen particles with respect to the temperature.

The corresponding relative time is also can be calculated in order to plot the quantity of desorbed hydrogen with respect to the time. The time was considered 0s at the beginning of the experiment and with the knowledge of the heating rate 0.3°C/s the time axis can be deducted from the temperature axis.

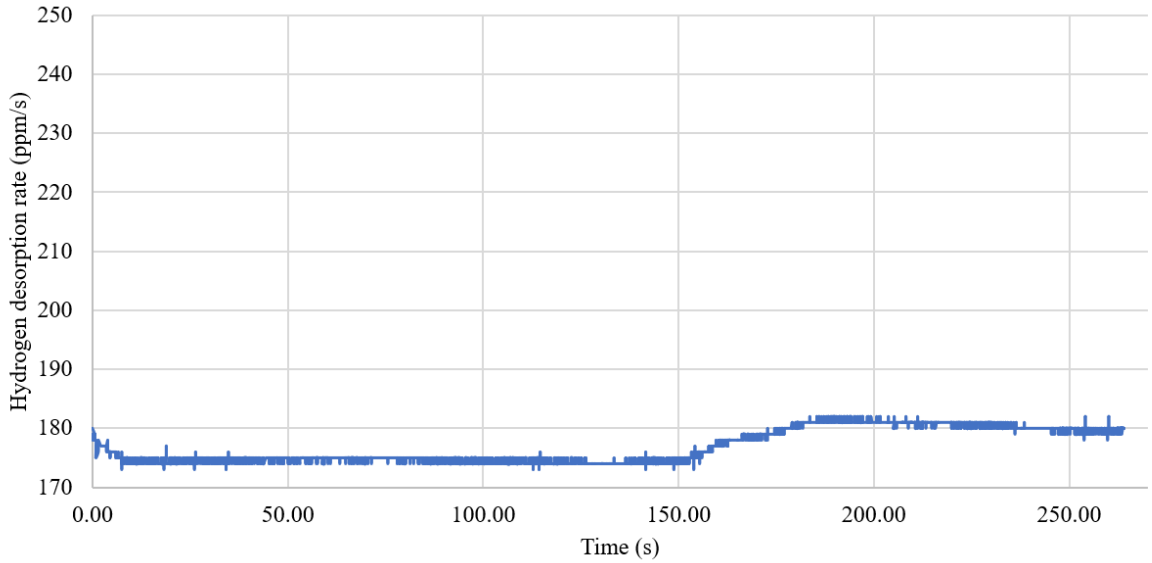

Figure 16: TDS curve of CP1180 without hydrogen charging, evolution of the quantity of desorbed hydrogen particles with respect to the time.

1.2. Experiment 2 _ CP 1180 (0.02mA/cm^2, 0MPa, 1h):

The sample CP1180 was subjected to thermal desorption and was charged under a charging current of 0.02mA/cm^2, a pressure of 0MPa and for 1h. Following the same process as previously we have these results:

Table 3: Results (Temperature, time, particle content) of the TDS of the CP 1180 steel with the conditions: 0.02mA/cm^2, 0MPa, 1h.

Temperature (^{o}C)	Particle content (ppm/s)
21	183
21	183
21	183
. . .	. . .
38	177
40	177
40	177
. . .	. . .
900	173
900	173
900	173

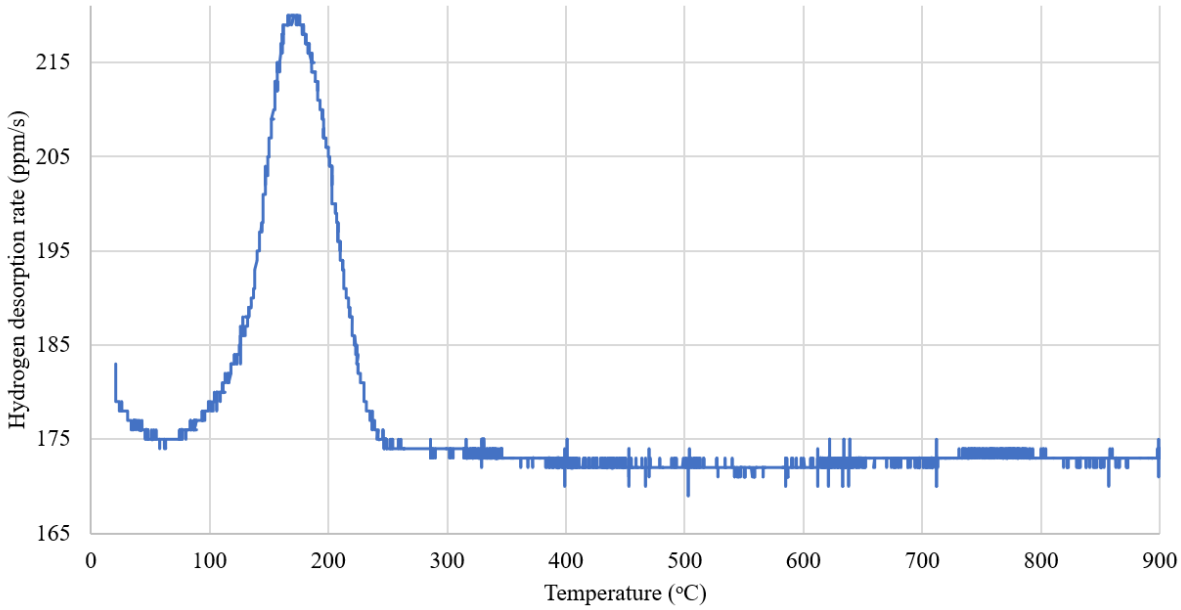

Figure 17: TDS curve of CP1180 with charging conditions: 0.02mA/cm^2, 0MPa, 1h , evolution of the quantity of desorbed hydrogen particles with respect to the temperature.

1.3.Experiment 3 _ CP 1180 (0.02mA/cm^2, 100MPa, 1h):

The sample CP1180 was subjected to thermal desorption was charged under a charging current of 0.02mA/cm^2, a pressure of 100MPa for 1h. Following the same process as previously we have these results:

Table 4: Results (Temperature, time, particle content) of the TDS of the CP 1180 steel with the conditions: 0.02mA/cm^2, 100MPa, 1h.

Temperature (°C)	Particle content (ppm/s)
21	183
21	183
21	183
. . .	. . .
38	177
40	177
40	177
. . .	. . .

900	173
900	173
900	173

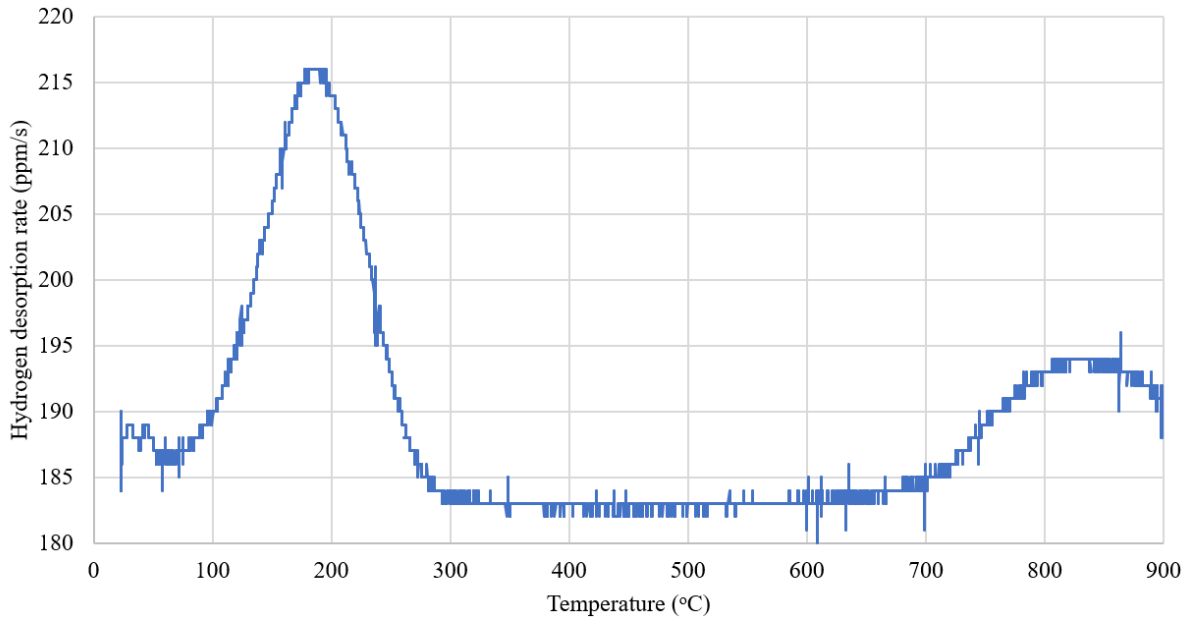

Figure 18: TDS curve of CP1180 with charging conditions: 0.02mA/cm^2, 100MPa, 1h , evolution of the quantity of desorbed hydrogen particles with respect to the temperature.

1.4. Experiment 4 _ CP 1180 (0.02mA/cm^2, 100MPa, 6h):

The sample CP1180 was subjected to thermal desorption was charged under a charging current of 0.02mA/cm^2, a pressure of 100MPa and for 6h. Following the same process as previously we have these results:

Table 5: Results (Temperature, time, particle content) of the TDS of the CP 1180 steel with the conditions: 0.02mA/cm^2, 100MPa, 6h.

Temperature (°C)	Particle content (ppm/s)
29	203
29	203
29	203
. . .	. . .
463	199

463	200
463	200
. . .	. . .
899	203
899	203
899	203

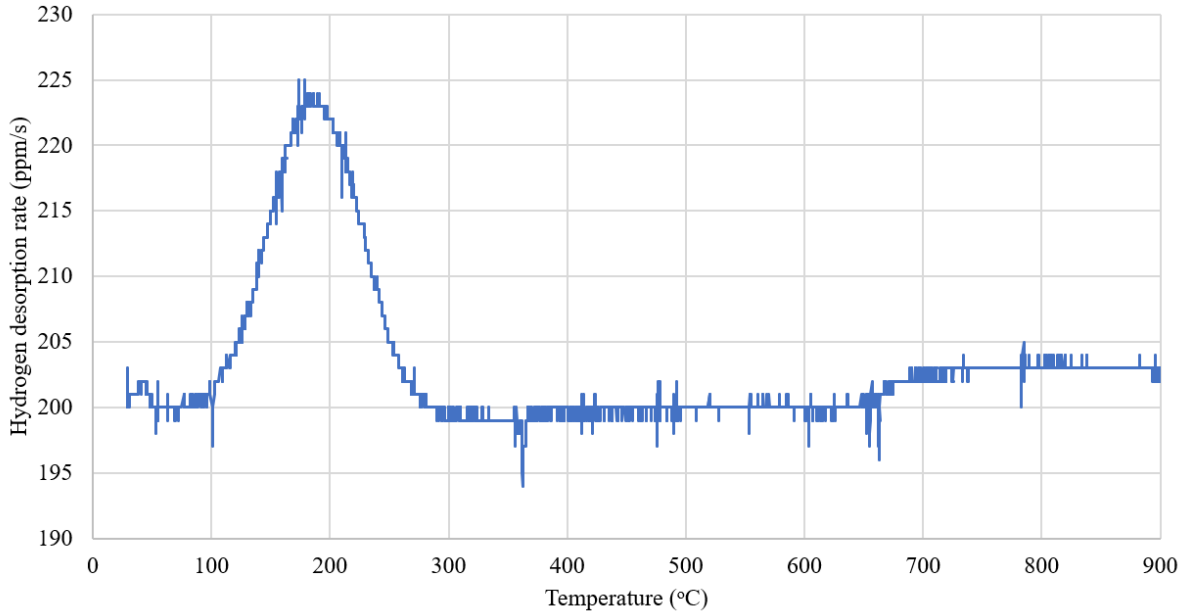

Figure 19: TDS curve of CP1180 with charging conditions: 0.02mA/cm^2, 100MPa, 6h , evolution of the quantity of desorbed hydrogen particles with respect to the temperature.

1.5.Experiment 5 _ CP 1180 (0.02mA/cm^2, 100MPa, 12h):

The sample CP1180 was subjected to the thermal desorption was charged under a charging current of 0.02mA/cm^2, a pressure of 100MPa for 12h. Following the same process as previously we have these results:

Table 6: Results (Temperature, time, particle content) of the TDS of the CP 1180 steel with the conditions: 0.02mA/cm^2, 100MPa, 12h.

Temperature (°C)	Particle content (ppm/s)

23	199
23	199
23	199
. . .	. . .
327	193
328	193
328	193
. . .	. . .
899	198
899	198
899	198

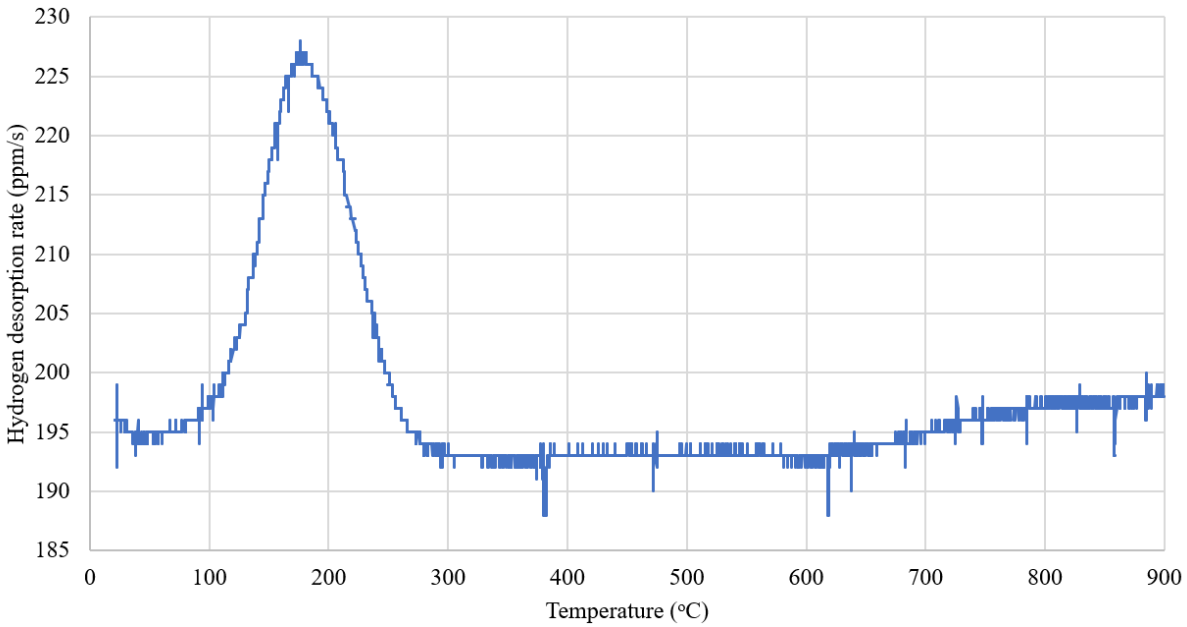

Figure 20: TDS curve of CP1180 with charging conditions: 0.02mA/cm^2, 100MPa, 12h , evolution of the quantity of desorbed hydrogen particles with respect to the temperature.

1.6. Experiment 6 _ CP 1180 (0.02mA/cm^2, 300MPa, 1h):

The sample CP1180 was subjected to the thermal desorption was charged under a charging current of 0.02mA/cm^2, a pressure of 300MPa and for 1h. Following the same process as previously we have these results:

Table 7: Results (Temperature, time, particle content) of the TDS of the CP 1180 steel with the conditions: 0.02mA/cm^2, 300MPa, 1h.

Temperature (^{o}C)	Particle content (ppm/s)
40	195
40	195
40	195
. . .	. . .
369	189
370	189
370	189
. . .	. . .
899	194
899	194
899	194

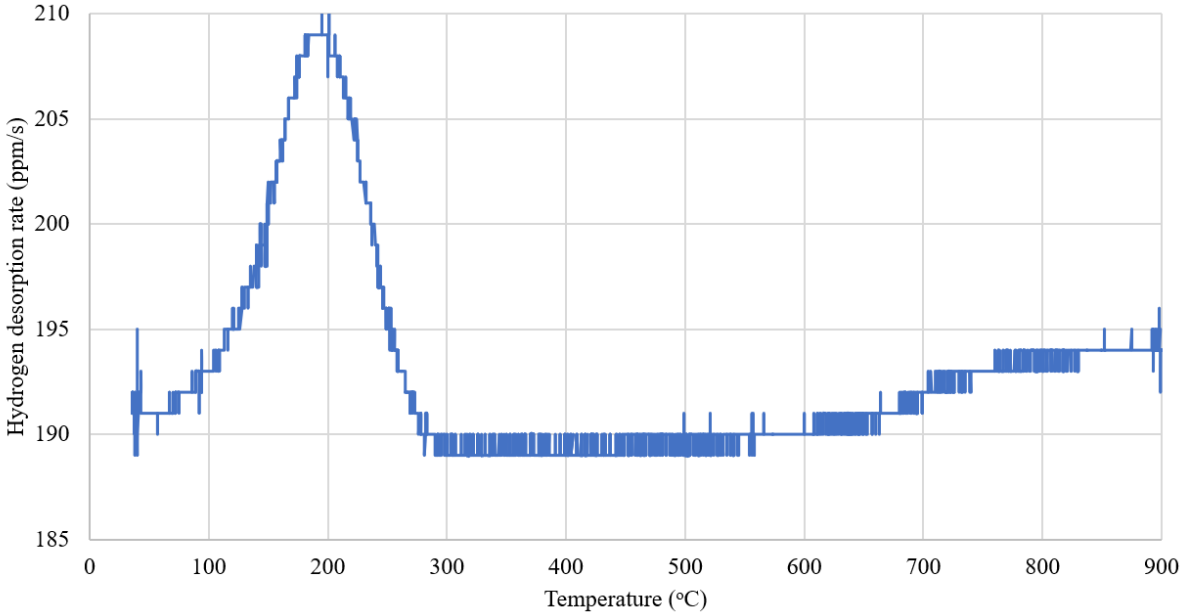

Figure 21: TDS curve of CP1180 with charging conditions: 0.02mA/cm^2, 200MPa, 1h , evolution of the quantity of desorbed hydrogen particles with respect to the temperature.

1.7. Experiment 7 _ CP 1180 (0.02mA/cm^2, 300MPa, 6h):

The sample CP1180 was subjected to the thermal desorption was charged under a charging current of 0.02mA/cm^2, a pressure of 300MPa and for 6h. Following the same process as previously we have these results:

Table 8: Results (Temperature, time, particle content) of the TDS of the CP 1180 steel with the conditions: 0.02mA/cm^2, 300MPa, 6h.

Temperature (°C)	Particle content (ppm/s)
34	204
34	204
34	204
. . .	. . .
501	204
503	204
503	204
. . .	. . .

900	208
900	208
900	208

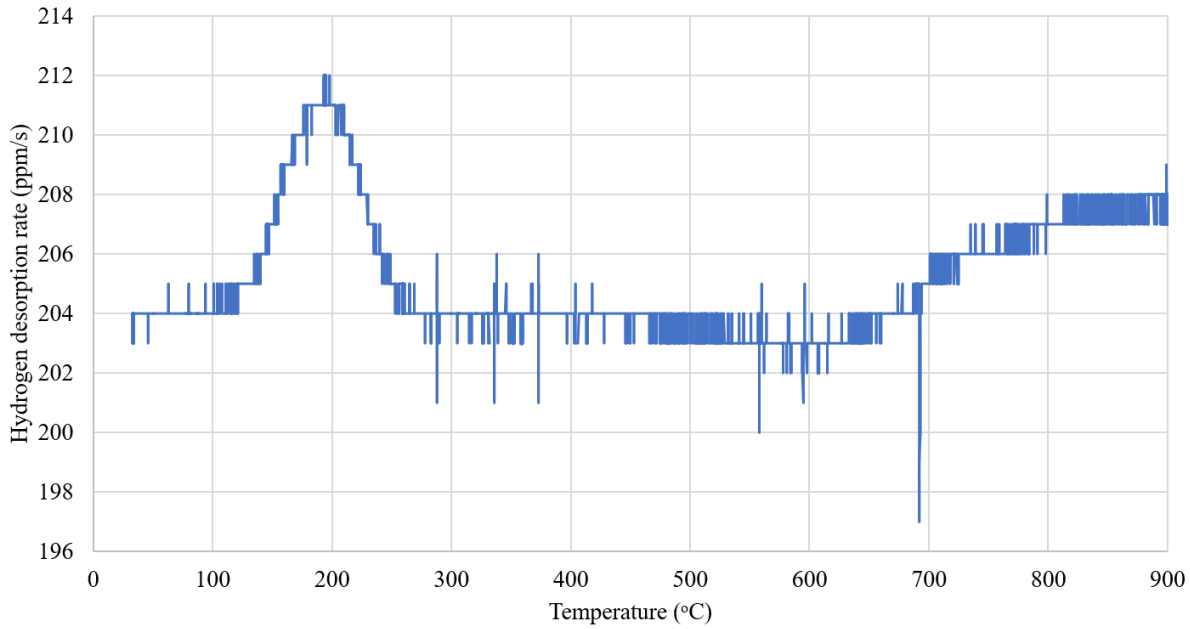

Figure 22: TDS curve of CP1180 with charging conditions: 0.02mA/cm^2, 200MPa, 1h , evolution of the quantity of desorbed hydrogen particles with respect to the temperature.

1.8. Experiment 8 _ CP 1180 (0.02mA/cm^2, 300MPa, 12h):

The sample CP1180 was subjected to the thermal desorption was charged under a charging current of 0.02mA/cm^2, a pressure of 300MPa and for 12h. Following the same process as previously we have these results:

Table 9: Results (Temperature, time, particle content) of the TDS of the CP 1180 steel with the conditions: 0.02mA/cm^2, 300MPa, 6h.

Temperature (°C)	Particle content (ppm/s)
23	203
23	203
23	203
. . .	. . .
535	196

535	196
535	197
. . .	. . .
900	201
900	201
900	201

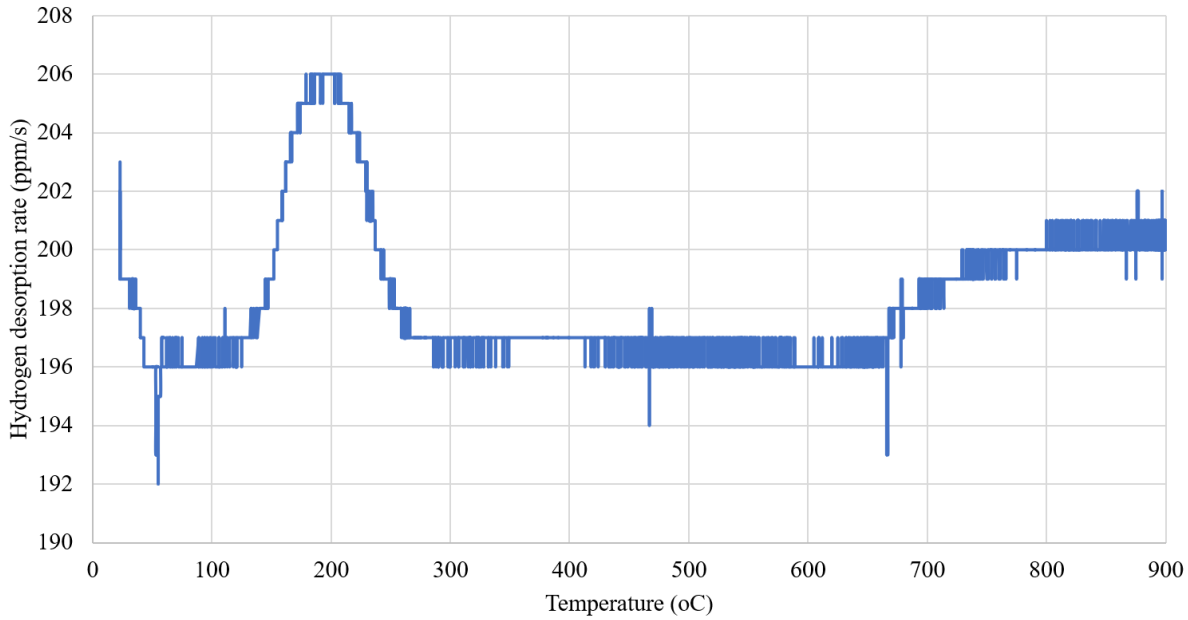

Figure 23: TDS curve of CP1180 with charging conditions: 0.02mA/cm^2, 200MPa, 1h , evolution of the quantity of desorbed hydrogen particles with respect to the temperature.

2. THERMAL DESORPTION SPECTROSCOPY: ANALYSIS AND DISCUSSIONS:

For the analysis of the results of the TDS, the influence of the different parameters involved in the hydrogen charging step will be discussed. Four different influencing parameters can be identified and discussed: the charging current density, the charging time, the pressure and the temperature.

To efficiently compare the results of the different experiments, the resulting plots are combined into one single plot as shown in **Figure 24**. For a more convenient analysis, they are titled as follows:

Experiment 1: ‘’P0_0h’’ means that neither pressure nor charging was conducted on this sample. Pressure 0MPa and charging time 0 hours.

Experiment 2: ‘’P0_1h’’ meaning a pressure of 100MPa and a charging time of 1h. The current density is the same for all the remaining experiments, the titles just mention those two parameters.

Experiment 3: ‘’P100_1h’’, experiment 4: ‘’P100_6h’’, experiment 5: ‘’P100_12h’’, experiment 6: ‘’P300_1h’’, experiment 7: ‘’P300_6h’’, experiment 8: ‘’P300_12h’’.

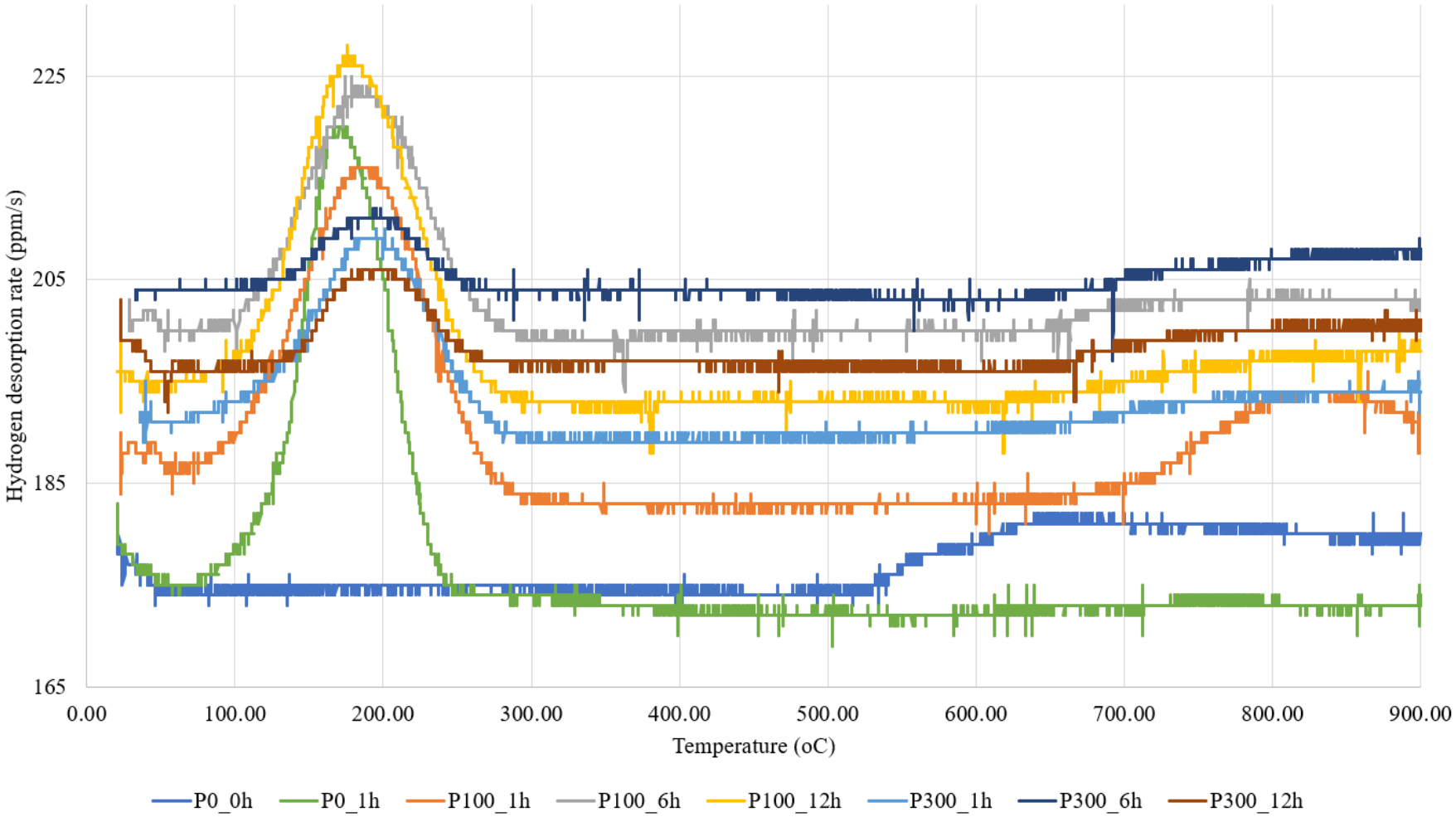

Figure 24: Comparison of TDS curves of the CP1180 sample in different test conditions, evolution of the quantity of desorbed hydrogen particles with respect to the temperature.

Following up, by using the heating rate which has been maintained constant to 0.3°C/s it is possible to change the temperature axis into a time axis. The resulting graph is revealed in **Figure 25**.

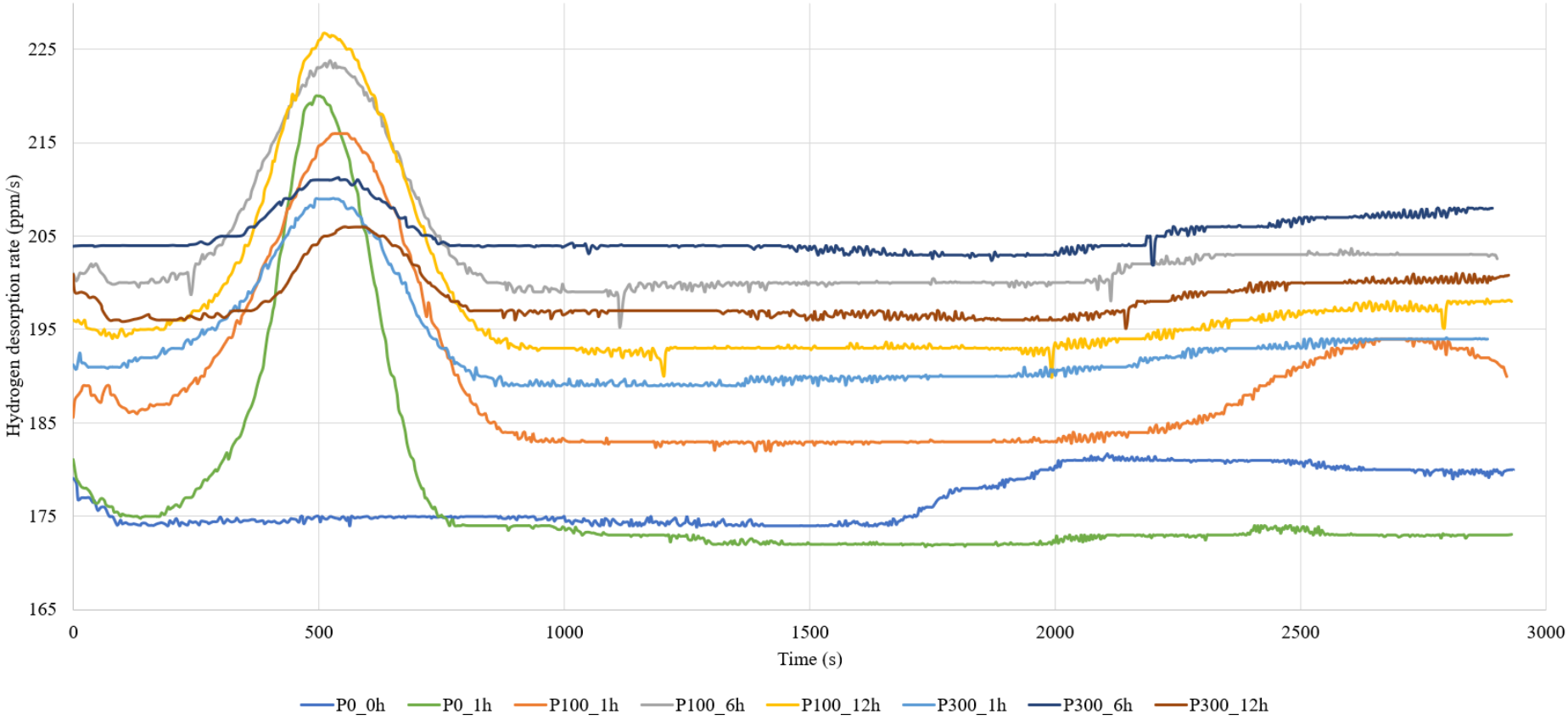

Figure 25: Comparison of TDS curves of the CP1180 sample in different test conditions, evolution of the quantity of desorbed hydrogen particles with respect to the time.

The upcoming discussion will be a qualitative and quantitative study of these plots.

2.1. The charging current density:

Based on the charging current density, the experiments can be categorised into two groups. Those without charging (experiment 1 without charging) and those with charging (all the 7 remaining experiments). There is clear evidence of the influence of the charging current density on the quantity of absorbed hydrogen. When analysing, it is seen that the plot ‘’P0_0h’’ is relatively flat with hydrogen particles' desorption rate varying between 173ppm/s and 180ppm/s while the range of variation of the other experiment is way larger. The **Table 10** highlights the key data of these plots.

The total amount of hydrogen for both samples in each case was also calculated and presented in **Table 10**. It is the surface area between the curve and the x-axis when the evolution is plotted with respect to the time (**Figure 25**). As there were two samples for each experiment, the average values will be the focus of the discussion. The experiment conducted without charging has a very low total hydrogen content as compared to the others.

Table 10: Maximum and minimum desorption rates of the different experiments and total amount of hydrogen absorbed.

	Desorption rates(ppm/s)		**Total absorbed hydrogen(ppm)**		
	Maximum	Minimum	Sample 1	Sample 2	Average
P0_0h	182	173	0.263510	0.322860	0.293185
P0_1h	220	169	0.800100	0.676270	0.738185
P100_1h	216	180	2.033780	2.869370	2.451575
P100_6h	225	194	2.863660	2.670620	2.767140
P100_12h	228	188	2.684990	4.129210	3.407100
P300_1h	210	189	1.218000	1.546460	1.382230
P300_6h	212	197	1.432330	1.989260	1.710795
P300_12h	206	192	1.288650	1.101310	1.194980

It is shown, from **Figure 25** that the current density during hydrogen charging has a significant influence on the absorption and desorption of hydrogen in steel. The experiment P0_0h is made without charging and shows a clear difference compared to the other experiments that were made with a charging density of 0.02mA/cm^2. The existence of a current is necessary for significant hydrogen charging and the higher the charging current density, the more hydrogen is absorbed. According to a study by X. Yang et al.(2022), a linear relationship

can be determined between the square root of the average hydrogen concentration and charging current density: $C \propto \sqrt{i_C}$[14] (proportional relationship).

In this study, X70 steel charging in a deep seawater environment was simulated. It was observed that the average hydrogen concentration increases with the charging current density.

Therefore, the relation between the absorbed hydrogen and the charging current density can be extended to the hydrogen environmental concentration. High hydrogen concentration conditions such as swamps, marshes, petroleum reservoirs, decaying plant material or organic waste and geological formations will lead to high absorption of hydrogen.

2.2. The charging time:

To analyse the impact of the charging time on the hydrogen content, the three plots ‘’P100_1h’’, ‘’P100_6h’’ and ‘’P100_12h’’. These experiments have been conducted under the same pressure and charging current density. The only parameter that has changed is the charging time.

The **Figure 25** shows that the higher the charging time the higher the hydrogen content. It is further demonstrated by the **Table 10** when the maxima and minima and more especially the total hydrogen absorbed quantities are compared: 2.451575 ppm < 2.767140 ppm < 3.407100 ppm (respectively the hydrogen absorbed by ‘’P100_1h’’, ‘’P100_6h’’ and ‘’P100_12h’’).

The duration of charging directly correlates with the length of time a sample is subjected to a hydrogen-rich environment, and the findings indicate that prolonged exposure leads to higher hydrogen absorption. Hence, it is crucial to evaluate the maximum amount of hydrogen a material can absorb before it reaches a critical point. This assessment depends on how the material will be used. Once we have this knowledge, we can determine safe periods for using the material. This prevents any harmful outcomes caused by the material absorbing too much hydrogen. These established safe time frames provide important information to guarantee the material works well and lasts a long time in real-world situations.

2.3.The pressure:

To discuss the influence of the pressure the analysis will be based on a pairwise comparative study of the data as follows:

Table 11: Pairwise comparative analysis of hydrogen particle content of samples with the same charging time but different pressure

Pressure (MPa) / Time (hours)	100	300
1	2.451575	1.38223
6	2.76714	1.710795
12	3.4071	1.19498

The **Table 11** shows that for each case, the hydrogen absorbed is less important as the pressure goes up. The pressure in this particular setup is outward-directed as the sample is elongated. In case of increasing inward pressure, the hydrogen absorption will have a higher rate and values[15].

It is also observed that the desorption rates are decreasing as the pressure goes up. This is explained by a less dense structure as the pressure increases outwards during the strain rate charging. Metals' reactivity and capacity to absorb hydrogen can be impacted by the hydrogen gas pressure. Metals absorb more hydrogen when the hydrogen gas pressure is higher[15]. In environments like deep ocean where the pressure and hydrogen concentration are high on the material, the hydrogen absorption can be expected to be significant.

2.4. The temperature:

One influencing parameter that is also analysed is the temperature. The **Figure 24** shows that the hydrogen desorption rate reaches its peak at a temperature of around 180ºC. That is considered the desorption temperature. The heat that is applied to the steel provides thermal energy to hydrogen atoms that end up desorbing from the metal when reaching here activation energy.

In real-world applications, like those in hydrogen fuel cell vehicles, industrial processes, and aerospace applications, the influence of temperature on CP1180 becomes a critical consideration. Achieving an efficient release of hydrogen from this material relies on recognizing the temperature factor. Elevating the temperature to approximately 180°C emerges as the key to optimizing the hydrogen desorption rate. This knowledge plays a pivotal role in shaping the design of processes and systems reliant on hydrogen release from CP1180.

When the temperature continues rising the desorption rate starts decreasing showing that the hydrogen content is also lowering till a point where there is no significant change in the desorption rate. However, the last stage, in all cases, is reached at extremely high temperatures,

around 600°C and more where the melted state is attained. It is observed a new increase in the desorption as the structure of the metal is fragile if not completely dissociated.

CONCLUSION:

The analysis of the various experimental results shows the impact parameters such as charging current density, which is directly related to the hydrogen concentration, the charging time or exposure period, the pressure and finally the temperature can have on the hydrogen absorption rate of steels, in this case, the CP1180.

The study has identified that a change in the hydrogen concentration in the surrounding of a material affects the charging current density which affects the rate at which it absorbs the hydrogen. The absorption rate increases when the inward pressure and the exposure time increase. Finally, the study of the properties through thermal desorption has demonstrated the hydrogen desorption pattern from the CP1180 when exposed to a variation of temperature.

The continuation of this work will propose a general conclusion in which the perspectives will be presented as to the use of these results and their implications.

CONCLUSION AND PERSPECTIVES

CONCLUSION AND PERSPECTIVES

The key findings of this study highlight the influencing factors that can affect how quickly steels absorb hydrogen and in which quantity. This includes charging current density, which is directly proportional to hydrogen concentration, charging duration or exposure period and lastly pressure. The influence of temperature on the rate at which hydrogen is desorbed by the metal is another characteristic that has been studied.

The discussion on the impact of these findings reveals that as pressure and exposure time rise, the absorption rate does as well. The pattern of hydrogen desorption from the CP1180 when exposed to a change in temperature has been shown by the investigation of the characteristics of thermal desorption. It increases with temperature and reaches its peak at 180^{o}C before dropping back.

By analysing the relation with the existing literature, it becomes clear that consideration has to be taken before choosing a material for a specific application depending on the environmental conditions the material will be exposed to. Thanks to the experiments conducted the effect of those conditions can be anticipated, leading to informed decisions.

This study successfully achieved the objectives outlined at the beginning of investigating the hydrogen absorption and desorption by high-strength steels with a focus on CP steels. This work comprehensively explored the hydrogen absorption properties of CP steels under varying conditions and analysed the desorption behaviour and provided practical comparison with natural existing conditions such as deep-water environments. The results obtained are in line with the specific aims set out in the introductory phase.

Despite the positive outcomes, this study does present certain limitations that warrant acknowledgement. It is important to recognize the constraints of this research that may have influenced the results obtained such as the lack of time to go through all the different experiments mentioned in the bibliographical review that could have brought several complementing information to the analysis of the impact of hydrogen on the material mechanical properties.

This opens up new avenues for further investigation into the impact of hydrogen on materials. The investigation can be pushed further by using the slow strain rate test to analyse how exactly CP1180’s mechanical properties like ductility, toughness, resilience and elasticity are affected by the different charging conditions.

In conclusion, this research has provided compelling evidence that a thorough evaluation and thoughtful consideration of the environmental conditions in which a material is intended

to be used can enable us to anticipate its response to hydrogen charging. By gaining this foresight, it becomes feasible to deduce appropriate economic, security, and safety measures aimed at averting potential failures or unfavourable outcomes. Thus, understanding the interplay between material behaviour and the surrounding environment is crucial for making informed decisions that promote both efficiency and safety in practical applications.

BIBLIOGRAPHIC REFERENCES

[1] S. Sorrell, “Reducing energy demand: A review of issues, challenges and approaches,” *Renew. Sustain. Energy Rev.*, vol. 47, pp. 74–82, 2015, doi: 10.1016/j.rser.2015.03.002.

[2] H. Ritchie, M. Roser, and P. Rosado, “Energy Production and Consumption,” *Our World Data*, 2022, doi: 10.1142/9789813148437_0009.

[3] M. Paranos and D. Marciu, “Hydrogen in energy transition : A review,” vol. 6, 2020, doi: 10.1016/j.ijhydene.2020.11.256.

[4] R. Moradi and K. M. Groth, “Hydrogen storage and delivery : Review of the state of the art technologies and risk and reliability analysis,” *Int. J. Hydrogen Energy*, vol. 44, no. 23, pp. 12254–12269, 2019, doi: 10.1016/j.ijhydene.2019.03.041.

[5] J. Sloan, “Composites end markets: Pressure vessels (2023),” 2023, [Online]. Available: https://www.compositesworld.com/articles/composites-end-markets-pressure-vessels-2023

[6] S. K. Dwivedi and M. Vishwakarma, “Hydrogen embrittlement in different materials: A review,” *Int. J. Hydrogen Energy*, vol. 43, no. 46, pp. 21603–21616, 2018, doi: 10.1016/j.ijhydene.2018.09.201.

[7] S. P. Lynch, “Hydrogen embrittlement (HE) phenomena and mechanisms,” *Stress Corros. Crack. Theory Pract.*, no. i, pp. 90–130, 2011, doi: 10.1533/9780857093769.1.90.

[8] M. Nagumo, *Manifestations of Hydrogen Embrittlement*. 2016. doi: 10.1007/978-981-10-0161-1_6.

[9] H. K. Birnbaum and P. Sofronis, “Hydrogen-enhanced localized plasticity-a mechanism for hydrogen-related fracture,” *Mater. Sci. Eng. A*, vol. 176, no. 1–2, pp. 191–202, 1994, doi: 10.1016/0921-5093(94)90975-X.

[10] A. Laureys, J. Van Stappen, T. Depover, V. Cnudde, and K. Verbeken, “Electrochemical hydrogen charging to simulate hydrogen flaking in pressure vessel steels,” *Eng. Fract. Mech.*, vol. 217, no. August, pp. 13–16, 2019, doi: 10.1016/j.engfracmech.2019.106546.

[11] J. Moverare, “Testing Methods for High Temperature Materials,” *Encycl. Mater. Met. Alloy.*, vol. 1, no. 0, pp. 277–286, 2021, doi: 10.1016/B978-0-12-803581-8.12106-X.

[12] A. Díaz, I. I. Cuesta, E. Martinez-Pañeda, and J. M. Alegre, “Analysis of hydrogen permeation tests considering two different modelling approaches for grain boundary trapping in iron,” *Int. J. Fract.*, vol. 223, no. 1–2, pp. 17–35, 2020, doi: 10.1007/s10704-

019-00411-8.

[13] C. D. Horvath, *Advanced steels for lightweight automotive structures*. LTD, 2020. doi: 10.1016/B978-0-12-818712-8.00002-1.

[14] X. Yang, F. Sun, Q. Li, R. Zhu, Z. Liu, C. Du, X. Li, "Effect of Hydrogen Charging on the Stress Corrosion Cracking Behavior of X70 Steel in Simulated Deep Seawater Environment," *Metals (Basel).*, vol. 12, no. 2, 2022, doi: 10.3390/met12020334.

[15] E. B. Taylor, 2013. "Effect of H_2 Pressure on Hydrogen Absorption and Granular Iron Corrosion Rates," Master Thesis, University of Waterloo.